AD-A108 419 COLLEGE OF WILLIAM AND MARY WILLIAMSBURG VA DEPT OF --ETC F/G 7/4
A STUDY OF THE COLLISIONAL DYNAMICS FOR COLLISIONS OF UF(6)(-) --ETC(U)
AUG 81 R L CHAMPION, L D DOVENSPIKE AFOSR-80-0227
UNCLASSIFIED UM AFOSR-TR-81-0742 NL

END
DATE FILMED
1 82
DTIC

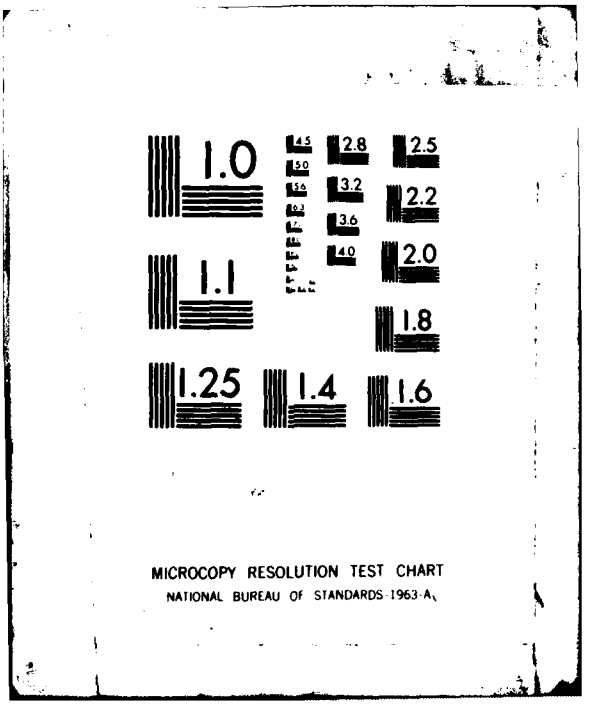
1.0
1.1
1.25
1.4
1.6
1.8
2.0
2.2
2.5
2.8
3.2
3.6
4.0
4.5
5.0
5.6
MICROCOPY RESOLUTION TEST CHART
NATIONAL BUREAU OF STANDARDS-1963-A

Report U4

FINAL SCIENTIFIC REPORT

for

AFOSR-[redacted] 80-0227

"A Study of the Collisional Dynamics for Collisions of UF_6^- with Atoms and Molecules"

R. L. Champion

L. D. Doverspike

Department of Physics

College of William and Mary

Williamsburg, Virginia 23185

August 1981

12 26

411978

Unclassified

SECURITY CLASSIFICATION OF THIS PAGE (When Data Entered)

REPORT DOCUMENTATION PAGE	READ INSTRUCTIONS BEFORE COMPLETING FORM
REPORT NUMBER AFOSR-TR- 81-0762	2. GOVT ACCESSION NO. AD A108419	3. RECIPIENT'S CATALOG NUMBER
4. TITLE (and Subtitle) A Study of the Collisional Dynamics for Collisions of UF(6) With Atoms and Molecules	5. TYPE OF REPORT & PERIOD COVERED Final; 1 July '80-30 June'81
	6. PERFORMING ORG. REPORT NUMBER
7. AUTHOR(s) R. L. Champion and L. D. Doverspike	8. CONTRACT OR GRANT NUMBER(s) AFOSR 80-0227
9. PERFORMING ORGANIZATION NAME AND ADDRESS Department of Physics College of William and Mary Williamsburg, VA 23185	10. PROGRAM ELEMENT, PROJECT, TASK AREA & WORK UNIT NUMBERS 61102F 2301/A8
11. CONTROLLING OFFICE NAME AND ADDRESS Air Force Office of Scientific Research Directorate of Physics Bolling AFB, DC 20332	12. REPORT DATE August 1981 13. NUMBER OF PAGES 20
14. MONITORING AGENCY NAME & ADDRESS(if different from Controlling Office)	15. SECURITY CLASS. (of this report) Unclassified 15a. DECLASSIFICATION/DOWNGRADING SCHEDULE

16. DISTRIBUTION STATEMENT (of this Report)

Approved for public release;
Distribution unlimited.

17. DISTRIBUTION STATEMENT (of the abstract entered in Block 20, if different from Report)

18. SUPPLEMENTARY NOTES

19. KEY WORDS (Continue on reverse side if necessary and identify by block number)

Collisional Decomposition of the Negative Ion of Uranium Hexafluoride

20. ABSTRACT (Continue on reverse side if necessary and identify by block number)

Absolute total cross sections for the collisional decomposition of the negative ion of Uranium Hexafluoride have been measured for laboratory collision energies up to 500 eV. The results have been analyzed with a statistical theory of unimolecular decomposition. By varying the temperature of the carbon surface upon which the negative ions are created, the average initial internal energy in the negative molecular ion can be selected. Experiments performed with "hot" negative molecular ions

on back

DD FORM 1 JAN 73 1473 EDITION OF 1 NOV 65 IS OBSOLETE

Unclassified

SECURITY CLASSIFICATION OF THIS PAGE (When Data Entered)

indicate larger decomposition cross sections and lower energy thresholds when compared to results for "cold" negative molecular ions.

A

TABLE OF CONTENTS

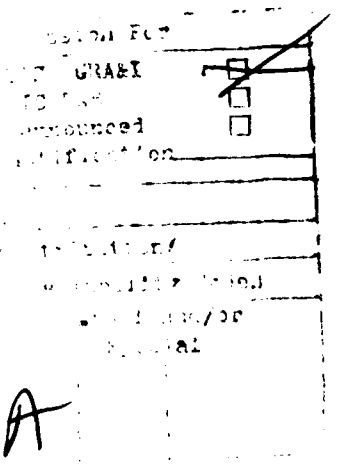

I. Introduction

The objective of this research project was to investigate the collisional dynamics associated with gas phase collisions of the negative ion of uranium hexafluoride, UF_6^-, with various atomic and molecular targets. The collisional energy range which was emphasized ranged from a few electron volts up to a (laboratory) energy in the vicinity of 1 keV. Thus, the energy range corresponds to the kinetic energies associated with ions typically found in an ion source. A secondary objective of this project was to study the process of surface anion formation, i.e., the mechanism whereby UF_6, after colliding with a hot surface, desorbs from the surface as a negative ion, UF_6^-. Both of these objectives were completed during the grant period.

These two objectives are somewhat distinct and it is perhaps useful to discuss them separately. In what follows we will first discuss the various mechanisms of collisional decomposition observed for UF_6^- ions, followed by a discussion of the surface electron attachment process in which the UF_6^- ion is created. The former aspect of the research effort has been published and that publication is attached to this report. The latter aspect has not yet been published.

II. Collisional Decomposition of UF_6^-

We have measured absolute total cross sections for the following processes:

$$UF_6^- + M \rightarrow UF_5 + F^- + M \quad (1a)$$

$$\rightarrow UF_5^- + F + M \quad (1b)$$

$$\rightarrow UF_6 + e + M \quad (1c)$$

where M = Ne, Ar, Kr, Xe, N_2, SF_6. The energy range for the experiments is from below the threshold for any of (1) up to around 0.5 keV. The experimental results and theoretical analyses for the rare gas targets, along with an extensive discussion of the experimental method, have been recently published in The Journal of Chemical Physics [J. Chem. Phys. 74, 2845 (1981)]. A reprint of this article is attached to this report as Appendix A. The salient features of the article are summarized below:

1. The collisional detachment cross section (1c) remains small for all the energies investigated, never exceeding 1 Å^2. This was completely unexpected as collisional detachment is usually the dominant inelastic process in collisions of negative ions with atoms or molecules.
2. On the other hand, the cross section for the production of F^- (1a) is large with a value of about 25 Å^2 for the largest target (Xe) and decreasing somewhat for the lighter targets. These results indicate that it may be feasible to use such stripping or decomposition channels for the generation of farily concentrated neutral beams of heavy particles.

3. Cross section measurements in the near-threshold region (i.e., low collision energies) indicate that the pre-collision UF_6^- ion may be created with an average internal energy which is in excess of that predicted if it is in thermodynamic equilibrium with the surface from whence it desorbs. This will be discussed in some detail later.
4. A model which uses a statistical theory of unimolecular decomposition was applied with considerable success, to the collisional decomposition of UF_6^-. The observed branching ratios for the exit channels in Eqs. (1) and their dependence upon energy were in remarkable accord with this statistical description.

The experiments described in Appendix A were extended to include the molecular targets, N_2 and SF_6 to see if there were substantive differences for the collisional decomposition of UF_6^- by molecular targets, as compared to atomic targets. The results for these two molecular targets are given in Fig. 1. At the highest relative collision energies available, the SF_6 target provides the largest decomposition cross sections observed. However, for SF_6, the branching ratio for collisional detachment at the highest collision energies is smaller than for any other target investigated, namely 1.6% of that for F^- production. In all other aspects, however, the results are rather similar to those observed for rare gas targets. In particular, the near-threshold behavior for (1c) and (1a) is almost identical to that observed with the rare gas targets.

The conclusion from these experiments is that the target serves merely as a spectator in the collisional excitation of UF_6^-. Although larger targets provide a larger cross section for excitation of the negative ion, the subsequent decomposition of the excited negative ion is governed by

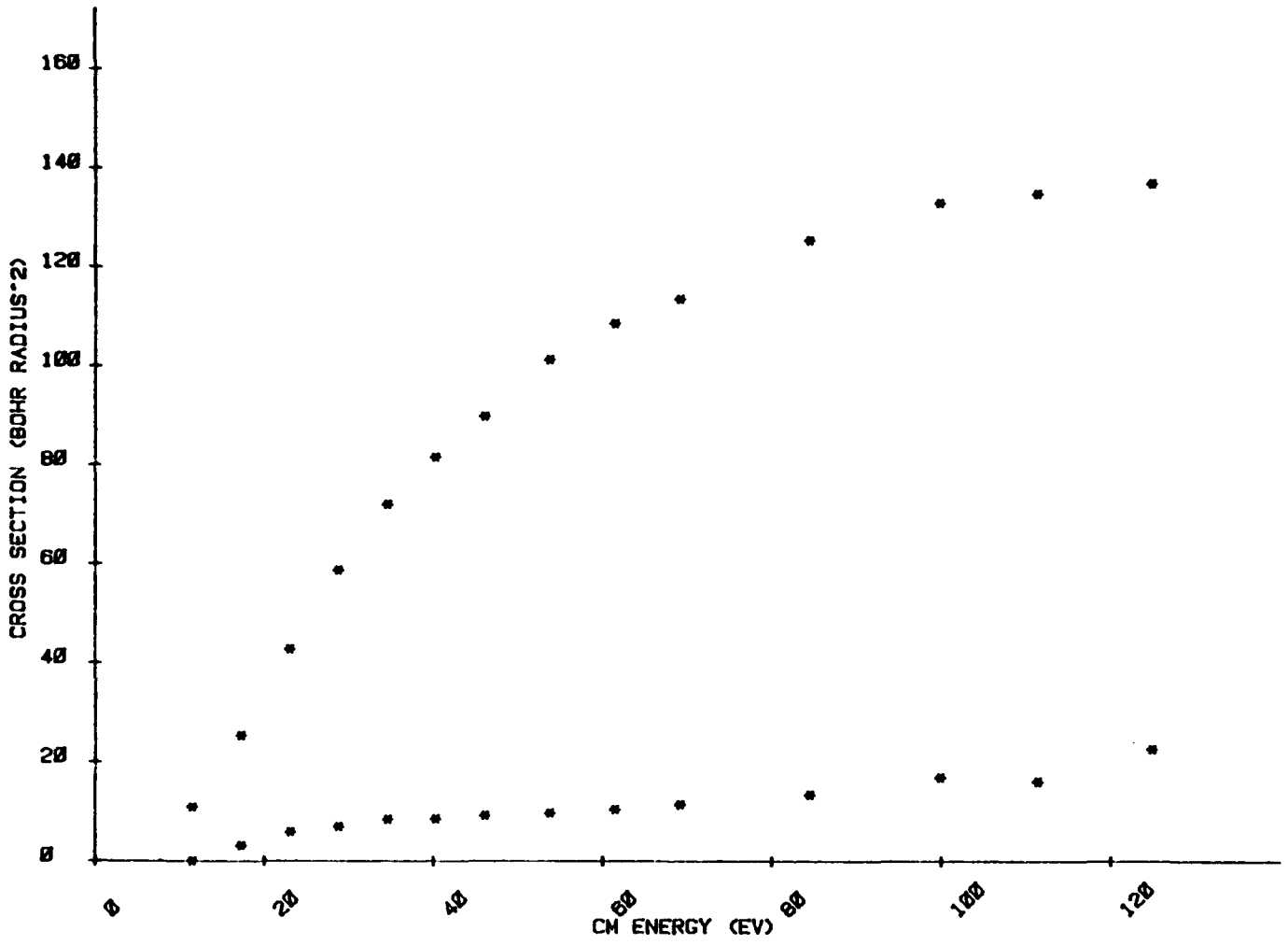

Fig. 1A. The cross sections for F^- and electron production are shown for the target SF_6. The lower curve is for electron detachment and has been multiplied by a factor of 10.

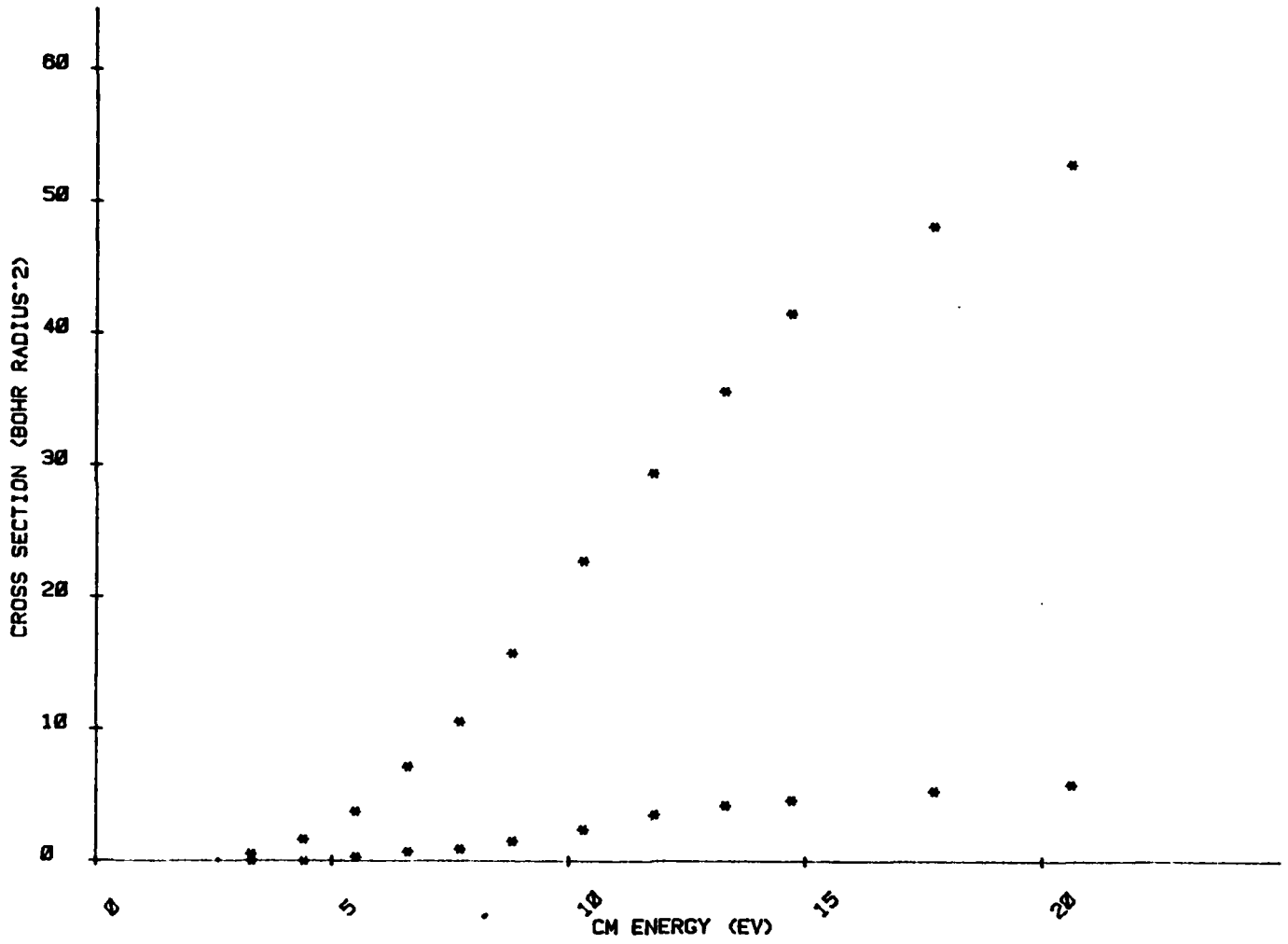

Fig. 1B. The cross sections for F^- and electron production are shown for the target N_2. The lower curve is for electron detachment and has been multiplied by a factor of 10.

statistical arguments which are independent of which target provided the collisional excitation. When the experimental cross sections are displayed in the center-of-mass coordinate system (as in all the figures contained herein), the cross sections exhibit almost identical behavior.

III. Ion Source Development and the Role of Internal Energy in Collisional Decomposition

The original ion source which was used in all of the previously discussed experiments employed a Platinum filament at 1230°K in a background gas of acetylene (C_2H_2) to produce the UF_6^- ion beam. The acetylene presumably rendered the surface "carbon-like" which was necessary to provide an inert surface upon which chemical decomposition of UF_6 was slow when compared to the residency time of the molecule on the surface. Thus, the UF_6 survives on such a surface and since the electron affinity of UF_6 is larger than the work function of this carbon-like surface, the UF_6 desorbs as an anion, UF_6^-. This arrangement was, however, not satisfactory for studying the detailed effects of surface temperature upon (i) the anion desorption efficiency and (ii) the effects of surface temperature (and hence the internal energy of the primary UF_6^- ion) upon the various decomposition cross sections.

Consequently, a filament of pure carbon was substituted for the platinum-C_2H_2 arrangement. This new filament was constructed from a piece of exfoliated graphite (from Union Carbide Corp., under the trade name of "Grafoil") which was 0.005" thick and about 0.25" wide. A filament constructed of such material was found to be quite ductile, very easy to work with and exhibited no embrittlement after extensive heating and simultaneous exposure to UF_6 vapor. More importantly, however, such a filament is long-lived, and provided a monoenergetic and copious beam of UF_6^- ions for a wide range of filament temperature.

Experiments at various filament temperatures were performed after an initial determination of the filament current vs. temperature curves for the "Grafoil" filament described above. This calibration was made with the filament in situ, i.e., located directly in the ion source mounting. This was done to avoid any effects due to geometry, clamping pressure or mounting hardware. Such a calibration curve is exhibited in Fig. 2.

The ion source which contained the carbon filament produced stable and intense UF_6^- ion beams with the filament operating over the temperature range from 225°C up to 1540°C. In order to investigate the possible role that internal energy plays in the collisional decomposition of UF_6^-, the cross section for F^- production (1a) was measured using ion beams which originated from surfaces of varying temperature. The surface temperature range which was investigated ranged from 225°C to 1540°C and the target species was argon. The results of these experiments are seen in Fig. 3. Qualitatively, the results are reasonable: increasing the average internal energy of the primary ion beam increases the decomposition cross section. The magnitude of the increase is substantial in the near-threshold region but amounts only to about 10% for the temperature extremes in the high energy (asymptotic) region.

It is of interest to examine the near-threshold region of Fig. 3 in more detail. Figure 4 illustrates this region with a plot of the square root of the cross section exhibited as a function of the relative collision energy (similar to Fig. 7, Appendix A). The figure shows the resulting cross section measurements for two filament temperatures, 330°C and 1320°C. The curve for the lower temperature is seen to be shifted approximately 1 eV (to higher collision energies) with respect to the results observed

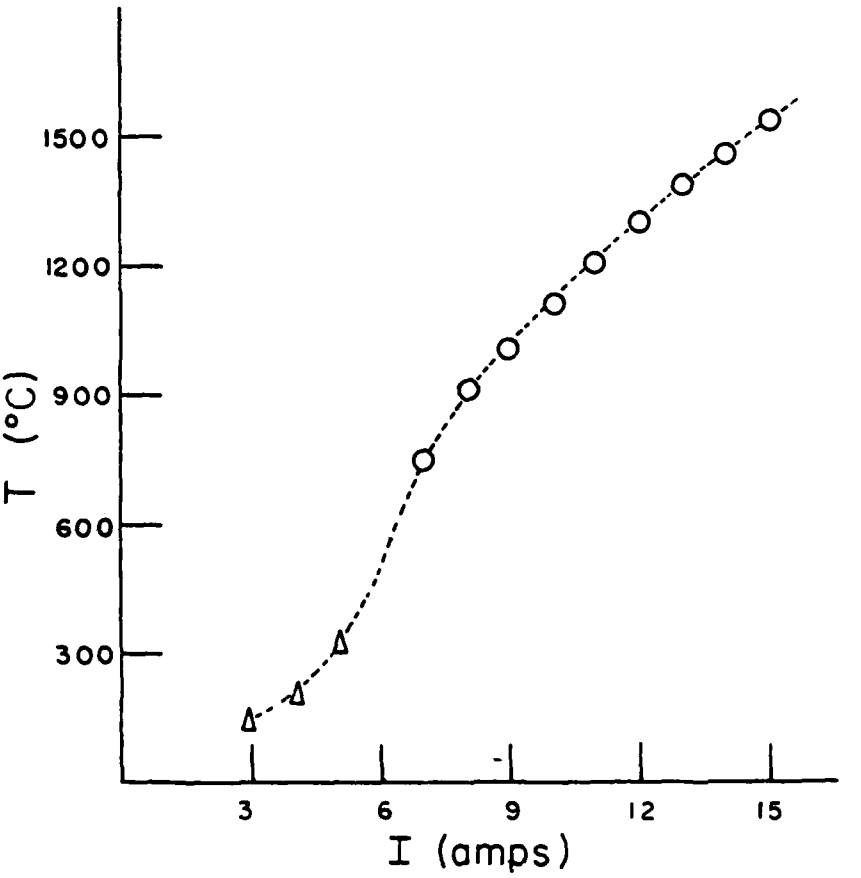

Figure 2. Calibration curve for "Grafoil" carbon filament used in UF_6^- ion source. The higher temperatures were determined by an optical pyrometer and the lower temperatures (triangles) were ascertained by a thermocouple.

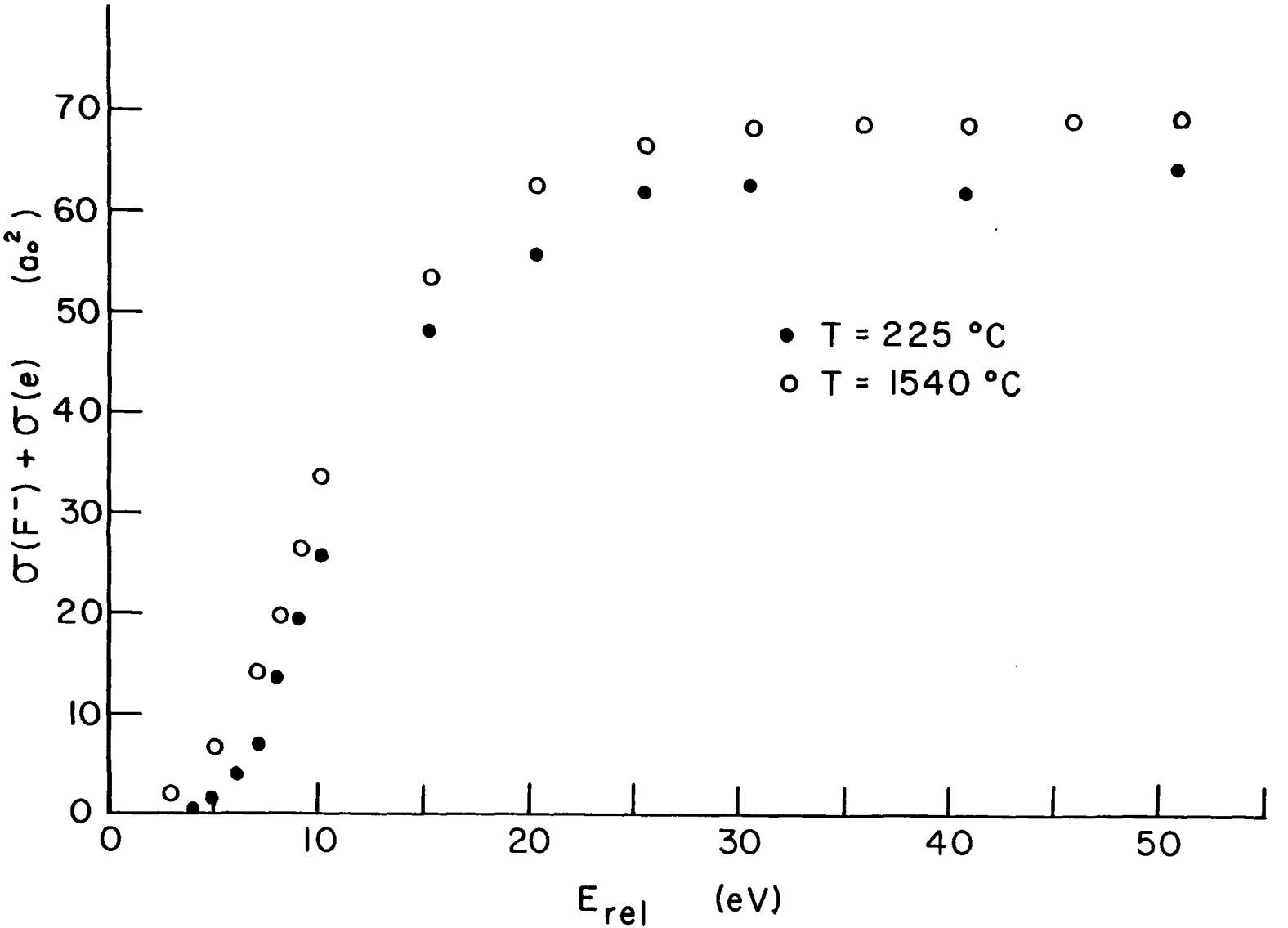

Figure 3. The sum of the detachment and the F^- cross sections (1a + 1c) are given as a function of the relative collision energy for an argon target. The results are for two different filament temperatures. Results for intermediate temperatures lie between those for the two temperature extremes plotted in the figure.

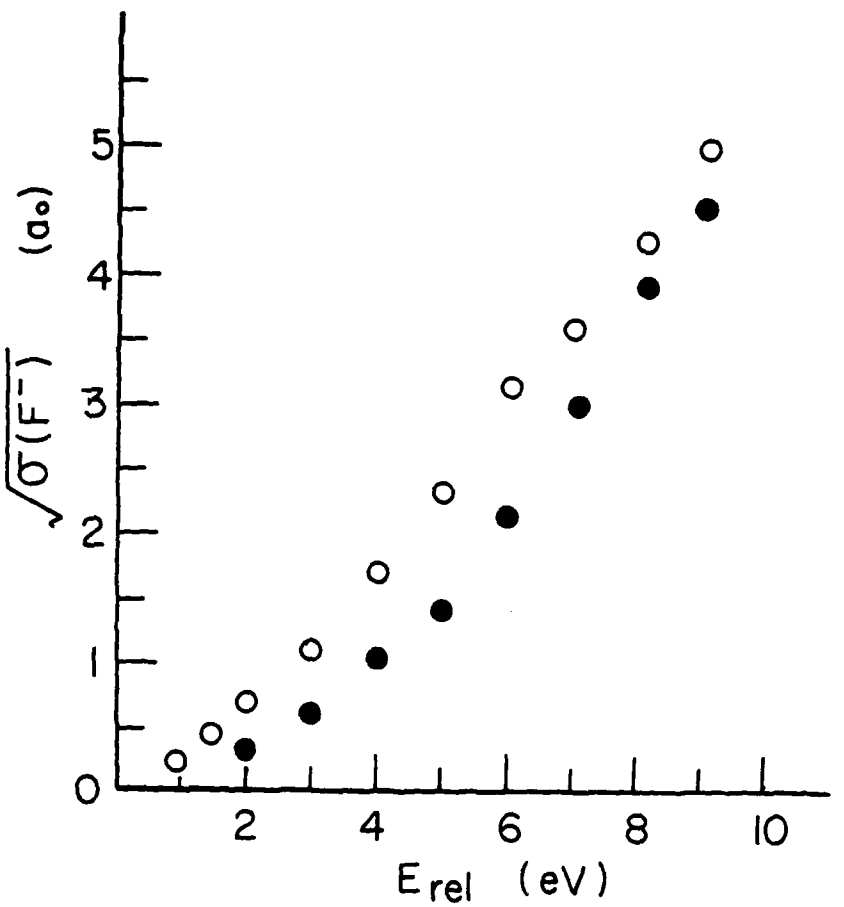

Figure 4. Near threshold behavior of $\sigma(F^-)$ as a function of relative collision energy is shown for two carbon filament temperatures; 1320°C (open circles) and 330°C (solid circles).

with the higher temperature filament. This shift of approximately 1 eV is the same as the anticipated change in the average internal energy of the desorbing UF_6^- ions if they desorb in thermodynamic equilibrium with the filament, viz., $U_{internal} \approx 15\ kT$ (see Eq. (3) App. A) and $\Delta U_{internal} \approx 15\ k\Delta T \approx 1.2$ eV for $\Delta T \approx 1000^{\circ}C$.

The low temperature threshold results continue to indicate an onset in the neighborhood of 2 eV or less. This low threshold for decomposition is incompatible with the generally accepted thermodynamics for UF_6^- (as given in Fig. 1, Appendix A). As mentioned earlier (in App. A) the effects of collisional broadening are small and, for the results of Fig. 4, any UF_6^- excitation within the ion source has been minimized by operating the source at a very low pressure. Hence, the reason for the apparently low threshold for F^- production is yet to be understood.

IV. Conclusion

The ease with which UF_6^- can be formed on a carbon filament (in particular, "Grafoil") of moderate temperature suggests that such an arrangement could be used efficiently as an ion source to generate intense beams of heavy negative ions. Applications which might utilize such ion beams include those of uranium isotope separation (using superconducting magnets, for example) and the generation of high energy, heavy neutral particle beams. The latter would require that the ion beam be neutralized at perhaps MeV kinetic energies where, presumably, the detachment cross section is considerably larger than it was found to be in our lower energy experiments.

If such ion source development is pursued, our absolute cross section measurements discussed herein will provide a starting point from which detailed design considerations and modeling may begin. This is due to the fact that typical kinetic energies found in ion sources include that range investigated in this study.

Several questions remain, however, before any serious considerations for ion source development could be launched. First, the question of "loading" the carbon filament with too much UF_6 (so that the anion conversion efficiency becomes substantially less than unity) has not been investigated. Secondly, to our knowledge, the various decomposition cross sections have not been measured at high collision energies. Both of these problems were outside the scope of our research objectives and program.

V. Personnel Associated with Research Effort

The following personnel have been associated with the research effort at William and Mary during the period July 1, 1980 - June 30, 1981:

S. E. Haywood*	2 Woman-months
M. Doverspike*	4 Man-months
M. S. Huq*	10 Man-months
R. L. Champion	3 Man-months
L. D. Doverspike	2 Man-months

*Graduate Student.

VI. Appendix

The following manuscript contains the details of a portion of the work performed during the grant period.

Collisional decomposition of UF_6^-

S. E. Haywood, L. D. Doverspike, and R. L. Champion

Department of Physics, College of William and Mary, Williamsburg, Virginia 23185

E. Herbst[a]

Department of Chemistry, College of William and Mary, Williamsburg, Virginia 23185

B. K. Annis and S. Datz

Chemistry Division, Oak Ridge National Laboratory, Oak Ridge, Tennessee 37830
(Received 28 August 1980; accepted 11 November 1980)

Absolute cross sections for the collisional decomposition of UF_6^- into its three lowest asymptotic channels in collisions with the rare gases have been measured for collision energies ranging from below the threshold for decomposition up to a laboratory collision energy of 500 eV. The product velocity spectra have also been measured for one of the decomposition channels at the highest collision energy. The experimental results are found to be consistent with the predictions of a two-step collision model where the unimolecular decomposition of excited UF_6^- ions is described in a statistical framework.

I. INTRODUCTION

Because of interests ranging from the separation of uranium isotopes to the production of electronless plasmas, uranium hexafluoride, UF_6, has been studied extensively both experimentally and theoretically.[1–12] There is now substantial evidence from surface ionization,[1] ion cyclotron resonance,[2] and ion-neutral beam experiments[3–6] to establish that uranium hexafluoride has a large electron affinity. The studies to date are consistent with a lower limit of $\simeq 5$ eV for the electron affinity of UF_6. It is likely that molecules with such large electron affinities possess a number of electronically excited bound states of the molecular negative ion. Recent calculations suggest the existence of such excited states for UF_6^- which lie within 3 eV of the $^2A_{2u}$ ground state.[9,10]

Experiments[12] involving the collisional excitation of UF_6^- by rare gas and hexafluoride targets show that substantial amounts of excitation energy can reside in the negative ion, although the experiments do not reveal how this energy is distributed among the electronic, vibrational, and rotational degrees of freedom of UF_6^-.

Very little information is available on how UF_6^- decomposes in collisions with gaseous targets. Clearly when a complicated molecular ion such as UF_6^- collides with an atom or molecule at collision energies in excess of a few tens of electron volts, many ways of breaking up UF_6^- become energetically possible. Figure 1 contains an energy level diagram of some of the lowest lying decomposition channels.

The purpose of this paper is to report on recent measurements[13] of the absolute total cross sections for the decomposition channels

$$UF_6^- + X \begin{cases} \rightarrow UF_6 + e^- + X & \text{(1a)} \\ \rightarrow UF_5 + F^- + X & \text{(1b)} \\ \rightarrow UF_5^- + F + X & \text{(1c)} \end{cases}$$

where X is Ne, Ar, Kr, and Xe. The collision energies range from below the threshold for each channel [except 1(c)] up to 500 eV laboratory energy. The thresholds for channels (1a) and (1b) have been determined. The experiments are carried out in an ion-beam, gas target apparatus. In addition, time-of-flight velocity spectra for channel (1b), taken at the upper end of the energy range, are also presented. The experimental observations are analyzed in terms of a two-step statistical model which employs the basic formulation of Klots.[14]

In Sec. II a discussion of the experimental procedures is presented. Section III contains the experimental results, and finally, the model used in the analysis of the data is presented and applied to the experimental results in Sec. IV.

II. EXPERIMENTAL METHODS

The experiments were performed using two different types of apparatuses. One, in which total cross-section measurements were made, is located at the College

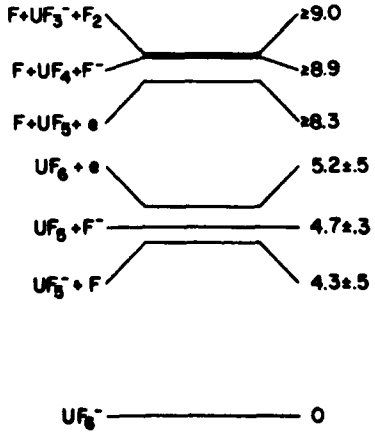

FIG. 1. Energy level diagram for the lowest decomposition channels of UF_6^-. The values are in electron volts and were obtained from Refs. 2 and 3.

[a] Present address: Department of Physics, Duke University, Durham, NC 27706.

 0021-9606/81/052845-06$01.00

of William and Mary and the other, in which the velocity spectra of the reaction products were obtained, is a time-of-flight apparatus located at Oak Ridge National Laboratory. One aspect of these experiments which is common to both apparatuses is the UF_6^- ion source. Consequently, we will first discuss the characteristics of this ion source and follow with a brief description of the separate apparatuses.

A. Ion source

The design of the UF_6^- source is based upon recent experiments of Dittner and Datz[1] in which they observed that UF_6 desorbed from a hot filament as a negative ion with a conversion factor (i.e., the ratio of the negative ion flux desorbing from the filament to the neutral flux which is incident upon the filament) which approached unity. Moreover, this conversion factor was observed to remain near unity over a wide temperature range, $500 \lesssim T \lesssim 2000$°K. This phenomenon is reasonable because the electron affinity of UF_6 (about 5.1 eV) is greater than the work function of the filament material. Thus, "surface attachment" for UF_6 molecules is an exoergic process. One further and crucial constraint is necessary, however, in order to achieve the unit conversion efficiency just mentioned. The surface of the filament must be such that the UF_6 molecules are not lost due to competing processes which may occur on the surface, such as $UF_6 \rightarrow UF_5 + F$, etc. A suitable "inert" surface was effected by using a platinum filament in a *background gas of* C_2H_2 (acetylene).[1] The surface is presumably carbon-like.

The ion sources employed in the present experiments used a platinum filament at a temperature of about 1230°K (as determined by an optical pyrometer) and a roughly equal mixture of C_2H_2 and UF_6 in the source chamber. Negative ion beams produced with this arrangement are both stable and intense. The total pressure within the ion source was not measured directly but is estimated to be in the neighborhood of about 10 μ. This estimate is based upon pressure measurements of the gas inlet tube on the upstream side of the actual source chamber. Because of the relatively high pressure within the source, some of the extracted UF_6^- ions may undergo inelastic collisions with the source gas before they reach the region of high vacuum (10^{-6} Torr) which is external to the ion source. The possible manifestations of such "collisional pumping" will be discussed after the experimental results are presented.

B. Total cross-section apparatus

The apparatus used to measure the various absolute total cross sections for Reactions (1) is only slightly modified from the one used in previous negative ion studies and is discussed in detail elsewhere.[15]

After the negative ion beam is extracted from the surface attachment ion source described above, it is accelerated and passes through a Wein filter and is subsequently focused into the collision chamber which contains the target gas; a schematic diagram of this chamber is given in Fig. 2. By varying electrostatic and magnetic fields within this collision chamber, it is possible to

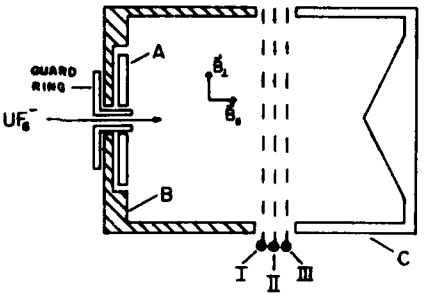

FIG. 2. Schematic digram of the collision chamber region. Grids labeled I, II, III are 95% transparent. By using grids II and III to provide retarding electrostatic fields and by applying either an axial ($B_\parallel$) or transverse ($B_\perp$) magnetic field, the three decomposition channels in Eq. (1) can be identified.

separate and measure the absolute total cross section for the three distinct reaction channels which are given in Eq. (1).

The collisional detachment (1a) is measured by applying an axial (i.e., along the beam axis) magnetic field of several gauss along with a small electrostatic field between grids I and II (see Fig. 2) to serve as an electron trap. All detached electrons must eventually be collected by the element A. The heavy F^- ions from Reaction (1b) will not be affected by the axial magnetic field, and some of those ions also arrive at element A. In order to separate the electron current from the F^- current, the magnetic field is rotated 90°. This will not affect the trajectories of the heavy negatively charged paricles but will prevent any electrons from reaching element A. Thus, the total electron current and hence the total detachment cross section can be ascertained. The initial UF_6^- beam current, the scattering path length, and the number density of scattering centers are known, and the cross section is unambiguously determined with an uncertainty estimated to be no more than 10%.

In order to discuss the measurement for channels (1b) and (1c), it is useful to assume that the dynamics of the collision-induced-dissociation (CID) channels [Reactions (1b) and (1c) above] can be qualitatively described by a two-step process:

$$\begin{aligned} UF_6^- + X &\rightarrow (UF_6^-)^* + X \\ &\quad\quad \vdash\!\rightarrow UF_5 + F^- \\ &\quad\quad \vdash\!\rightarrow UF_5^- + F \ , \end{aligned} \tag{2}$$

where the asterisk implies that $(UF_6^-)^*$ has been collisionally excited and contains sufficient internal energy so that the dissociation is energetically possible. The products of CID then have roughly the same velocity in the laboratory reference frame but quite different kinetic energies. It is this latter feature which allows one to separate channels (1b) and (1c).[16] For example, if the laboratory energy of the projectile UF_6^- is E_1(eV), then the laboratory kinetic energy for F^- resulting from CID will be about $E_1/17$. Consequently, if the voltage on grid II (see Fig. 2) is, say $E_1/8$ (volts), then all of the F^- which is due to CID will be reflected by that electric field and collected on elements A and B. The result of

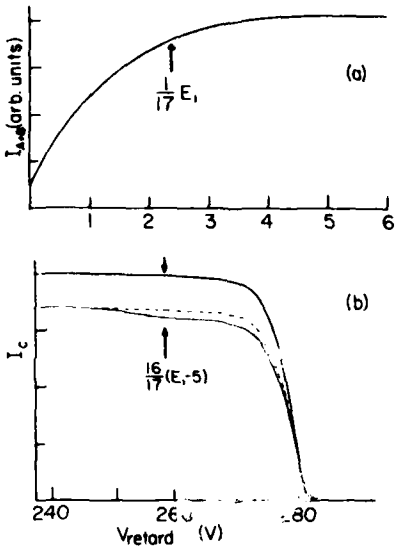

FIG. 3. (a) Retardation analysis for F^-; the ordinate gives the current to elements *A* and *B* as a function of a retarding voltage applied to grids II and III for the Xe target and a laboratory energy E_1 of 40 eV. The arrow at $V \simeq E_1/17$ is the mean energy (in electron volts) for F^- expected from simple CID considerations. (b) Retardation analysis for UF_5^-. The ordinate gives the current to element *C* as a function of the retarding voltage for the Ar target with $E_1 = 278$ eV. The arrow at $V \simeq 16\,(E_1 - 5)/17$ is the mean energy (in electron volts) for UF_5^- expected from simple CID considerations and an endothermicity of 5 eV in the original excitation process. The uppermost curve is a retardation plot for UF_6^- with no target gas in the collision chamber.

a "retardation analysis" is shown in Fig. 3(a). The observation of a plateau region clearly indicates that the reflection of the F^- ions is complete. Thus, the CID cross section for (1b) may be determined. The cross section for (1c) may also be measured in a similar fashion by varying the retardation voltage and observing the current which is transmitted through the retarding grids and collected on element *C*.

It is clear that the measurements can not unambiguously identify and separate the various heavy (charged) reaction products. Moreover, the simple two-step model which is used to discuss the kinematics of CID is probably overly simplistic. Nevertheless, any plausible modification of this model would not result in any substantial alteration in the kinematics of CID. Based upon the assumption that (1b) and (1c) are the sole products of CID, then the measurements for (1b) and (1c) should be accurate to within 10% and 30%, respectively. The larger error for (1c) is due to the fact that the larger retarding voltages, which are necessary to separate (1c) from elastic scattering (or the primary ion beam), cause a substantial defocusing of the ion beam which in turn makes the identification of "breaks" in the retardation analysis difficult to measure. Such a retardation is seen in Fig. 3(b). The uppermost curve in Fig. 3(b) is a plot of the current transmitted through the collision chamber without scattering gas as a function of the retarding voltage. The bottom curve is for the case where the scattering gas is admitted to the chamber. The dashed line is constructed to be parallel to the upper curve and corresponds to the hypothesis that the cross section for producing UF_5^- is zero. The difference between this hypothetical curve and the bottom curve yields the cross section for the UF_5^- channel.

The laboratory energy of the primary ion beam is determined by a retardation analysis similar to that shown in Fig. 3(b) with no target gas in the chamber. The scattering chamber is housed in a differentially pumped section which is well isolated from the ion source region. This arrangement minimizes UF_6 intrusion into the collision chamber, and no appreciable error owing to contact potentials should be present. The laboratory energy should be accurate to within 0.25 eV which translates into a very small error in the relative collision energy (i.e., the energy in the center-of-mass coordinate system) for the reactants studied.

C. Time-of-flight apparatus

The time-of-flight study was carried out on an apparatus which, apart from the installation of a carbon-coated filament as described above, was identical to that used for Cl^- collision studies and has been described in detail elsewhere.[17] In the present experiment a chopped UF_6^- beam with a laboratory energy of 500 eV was directed at a liquid-nitrogen-cooled scattering cell. Neutral particles produced in the UF_6^-–rare gas collisions traversed a 1 m path and were detected by a channeltron electron multiplier. The angular resolution of the apparatus was approximately 0.2° and the angular range ±3.5° could be scanned. The velocity spectra and energy-loss spectra for the scattered products were determined by measuring the time delays (referenced to the centroid of the primary UF_6^- distribution) for the scattered products.

III. RESULTS

A. Electron detachment cross sections

The absolute electron detachment cross sections for collisions of UF_6^- with the rare gases Ne, Ar, Kr, and Xe have been measured from threshold to a laboratory energy of 500 eV and the results are presented in Fig. 4. All the cross sections have the same general shape;

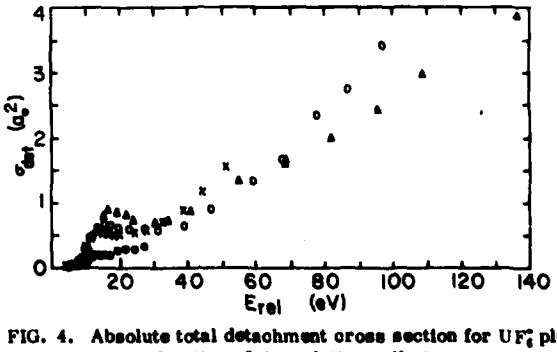

FIG. 4. Absolute total detachment cross section for UF_6^- plus rare gases as a function of the relative collision energy: △ Xe; ○ Kr; × Ar; ● Ne. The cross sections are in atomic units, $a_0 = 0.529 \times 10^{-8}$ cm.

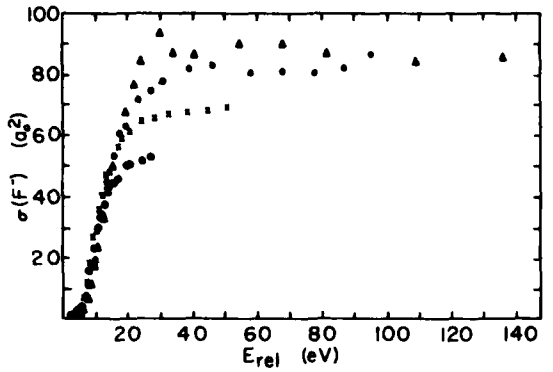

FIG. 5. Absolute total cross section for CID of UF_6^- by the rare gases as a function of the relative collision energy: Δ Xe; ○ Kr; × Ar; ● Ne.

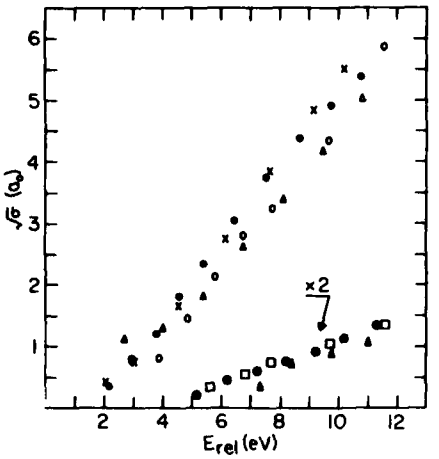

FIG. 7. Threshold behavior of $\sigma(F^-)$ and the detachment cross section. The square root of the cross sections are plotted as a function of the relative collision energy. (F^-): Δ Xe; ○ Kr; × Ar; ● Ne. Detachment: ▲ Xe; □ Kr; ⊗ Ar. The square root of the detachment cross section has been multiplied by two for display purposes.

each shows a threshold in the vicinity of 5 eV (their threshold behavior will be discussed in detail later), then rises to a local maximum at a relative collisional energy around 15 eV. Above 15 eV the cross sections decrease, and each (except for Ne) possesses a local minimum near 30 eV. Afterwards they increase monotonically with increasing collision energy. The low energy maximum in the cross section becomes more pronounced as the target mass increases, being almost indiscernable in the case of Ne.

This particular structure in the detachment cross section near threshold which is essentially independent of the target species is not understood at present. It should be noted that the detachment cross sections are remarkably small even at relative energies of 100 eV.

B. Dissociation channels

Absolute cross sections for the dissociation channels (1b) and (1c) were determined for the rare gas targets and same range of collision energy as for detachment. Cross sections for the product F^-, $\sigma(F^-)$, are presented in Fig. 5 while the ratio $\sigma(UF_5^-)/\sigma(F^-)$, rather than $\sigma(UF_5^-)$, is shown in Fig. 6. An interesting feature in Fig. 6, is that the ratio $\sigma(UF_5^-)/\sigma(F^-)$ is independent of the target and is an approximately universal function of the relative collision energy. Channel (1b), although more endoergic than (1c), is clearly the dominant process at elevated energies with (1c) becoming relatively important only in the threshold region. The data in Fig. 5 show that $\sigma(F^-)$ rises rapidly from a threshold in the vicinity of 2.5 eV then reaches a plateau for $E_{rel} \simeq 20$–25 eV. The cross sections also systematically increase with the mass of the target atom. These results show that electron detachment is a minor contributor to the collisional destruction of UF_6^- in the energy range investigated.

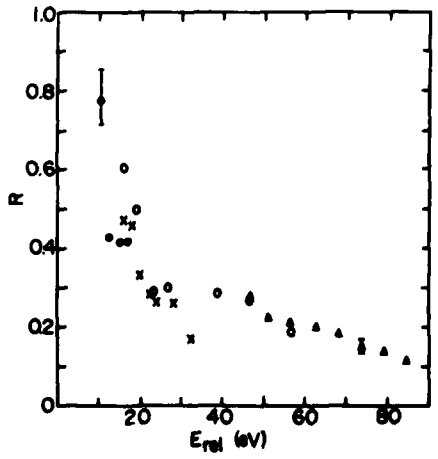

FIG. 6. Branching ratio for the two CID channels, where $R = \sigma(UF_5^-)/\sigma(F^-)$, as a function of the relative collision energy: Δ Xe; ○ Kr; × Ar; ● Ne.

C. Threshold measurements

The threshold region for Reaction (1b) was studied in detail for all the rare gas targets. Experimental limitations discussed earlier prevented similar measurements on channel (1c), while the smallness of the detachment cross sections limited the accuracy of threshold studies for this channel.

An expanded view of the measurements in the threshold region for channels (1a) and (1b) is shown in Fig. 7. For both channels the square roots of the cross sections are plotted versus relative collision energy, and it is clear the plots are quite linear over the range of energies shown. A linear extrapolation of $[\sigma(F^-)]^{1/2}$ to zero cross section indicates that the threshold for channel (1b) is approximately 2 eV for all targets, and the same procedure for the detachment channel (1a) is consistent with a threshold in the vicinity of 4–5 eV.

The observed threshold for process (1b) is considerably below the currently accepted value of 4.7 eV shown in Fig. 1. There are several reasons for expecting the threshold determined in the present experiments to be

lower. To begin with, the UF_6^- is produced by desorption from a hot filament and therefore will possess a significant amount of internal energy if it is in thermal equilibrium with the filament before desorption. All the data shown in this paper were taken at a filament temperature of 1230°K as determined by an optical pyrometer. Assuming the UF_6^- is in thermal equilibrium with the filament at temperature T, it then follows that the mean internal energy of the desorbed ions is

$$\bar{U} = \tfrac{3}{2}RT + \sum_{i=1}^{15} \frac{h\nu_i}{\exp(h\nu_i/kT - 1)} , \tag{3}$$

where the first term is the rotational contribution and the second is the energy in vibration. Using the estimates of Compton[3] for the vibrational frequencies ν_i of UF_6^-, Eq. (3) gives $\bar{U} = 1.5$ eV at a temperature of 1230°K. Assuming that UF_6^- contains this amount of internal excitation, one still needs an additional 1.2 eV in the form of internal excitation to explain the observed threshold for (1b). The experimental data have been corrected for thermal[10] and apparatus broadening by employing a numerical deconvolution scheme used in the analysis of previous threshold measurements[15] of collisional detachment cross sections. The effect of removing the broadening from the present data is quite small. The thresholds would be lowered by only about 0.1 eV and, therefore, cannot account for the 1.2 eV. One further source of broadening is due to the width of the distribution of excited states for the desorbing UF_6^- ion. This width can be on the order of $\bar{U}$ and hence may account for the rather low threshold observed in Fig. 7. An additional mechanism for producing UF_6^- ions with $U > \bar{U}$ is the "collisional pumping" of UF_6^- as it is extracted from the surface source. The extraction electrode extends approximately 2 cm inside the source chamber and is normally maintained at +100 V with respect to the filament and source chamber. With the present arrangement the source gas pressure is roughly the same throughout this region; the pressure, although not measured directly in the source, is probably high enough to make collisions between the extracted UF_6^- and UF_6 likely in the extraction region. Recent studies by Annis and Stockdale[12] show that when UF_6^- is scattered by various targets (including UF_6), $(UF_6^-)^*$ ions with several electron volts of internal energy and lifetimes $\gtrsim 45$ μsec are produced. Since the transit time in the present experiments is ~10 μsec, these collisionally excited UF_6^- ions are in the ion beam and are probably responsible for the low threshold observed. As can be seen in Fig. 7, the threshold for detachment is found to be several electron volts higher than that for F^- produced via CID, although the asymptotic states for the two channels are separated by only 0.5 eV. It will be shown later that this observation is compatible with the prediction of a statistical model; that is the lifetime for detachment of $(UF_6^-)^*$ is greater than the transit time within the collision chamber (~1 μsec) for low relative collision energies, in contrast to the prediction for CID.

D. Velocity spectra

Velocity spectra of the energetic neutral products of collisional decomposition were measured at a laboratory energy of 500 eV for laboratory scattering angles

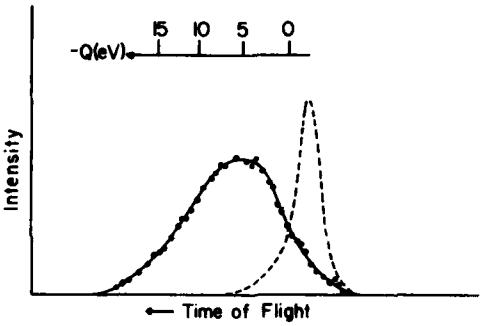

FIG. 8. Time-of-flight spectrum of UF_5 produced by UF_6^- in Ar for a laboratory energy of 500 eV and a laboratory scattering angle of 1.5°. Solid curve is UF_5 and the dashed curve is the primary beam UF_6^- profile. Also shown is the endothermicity $-Q$ for this process, determined by assuming that the CID can be described by a two-step model. See the text for discussion of the two-step model.

$\theta \leq 3.5°$. The particle detector in the time-of-flight apparatus would only detect UF_6 from channel (1a) or UF_5 from channel (1b). The F from channel (1c) would be detected with a much lower efficiency because of its low laboratory kinetic energy (approximately 30 eV). Since the total cross section for detachment is only a few percent of that for CID, the neutral time-of-flight (TOF) spectra essentially reflect the velocity spectra for channel (1b). An example for the Ar target is shown in Fig. 8 for a laboratory scattering angle of 1.5°. The scale at the top of the graph gives the endothermicity Q, calculated from the observed delay time for the UF_5 molecules, and is based upon the assumption of the two-step model:

$$\begin{aligned} &UF_6^- + Ar \rightarrow UF_6^{-*} + Ar + Q , \\ &UF_6^{-*} \rightarrow UF_5 + F^- , \end{aligned} \tag{4}$$

where in the second step the CID products separate from each other with negligible relative velocity and have a negligible postexcitation interaction with the neutral target atom.

If the CID products separate with nonzero momenta in an isotropic manner, then the net effect will generally be to broaden the velocity spectrum rather than to shift its centroid an appreciable amount. Hence, the centroid of the distribution in Fig. 8 that yields $\bar{Q} \simeq -5$ eV should be the endothermicity of the first step of CID if the assumptions of the two-step model are compatible with the reality of the collisional dynamics.

If $\bar{Q} \simeq -5$ eV, then the internal energy $\bar{U}$ of $(UF_6^-)^*$ for those molecular ions which ultimately decompose to $UF_5 + F^-$ is the sum of the internal energy prior to the collision and the 5 eV transferred by the collision. If the original internal energy of the UF_6^- projectile is about 2 eV (as indicated by the threshold behavior of the total CID cross section), then it follows that $\bar{U} \simeq 7$ eV for Reaction (1b) to occur. This result is compatible with the internal energy necessary to produce the observed CID branching ratio as predicted by the statistical theory to be discussed later. The velocity spectra taken with other targets are essentially the same as that shown in Fig.

8. The observed $\bar{Q}$'s are also approximately independent of scattering angle, and only a broadening of the velocity spectrum is observed with increasing scattering angle.

IV. THEORETICAL TREATMENT

We shall again assume that the collision-induced dissociation of UF_6^- can be approximated by the following two-step process:

$$UF_6^- + X \rightarrow (UF_6^-)^* + X \ ,$$

$$(UF_6^-)^* \rightarrow \text{products} \ ,$$

where X is a rare gas target. The first step is a strongly inelastic collision in which sufficient energy is transferred from the relative collision energy E_{rel} into internal energy of UF_6^- so that the molecule is excited into its quasibound rovibrational levels above at least the first dissociation limit. The second step is the subsequent dissociation of the $(UF_6^-)^*$ "complex." This description has meaning if the complex lifetime is greater than the collision time. The treatment here is concerned solely with the spontaneous decomposition of $(UF_6^-)^*$ molecules with known internal energy U and angular momentum quantum number J_0. We are able to calculate the $(UF_6^-)^*$ decomposition frequencies and relative strengths for the product channels, or branching ratios, as functions of U and J_0. We have not attempted to calculate the U and J_0 distributions of $(UF_6^-)^*$ species to be expected from $UF_6^- - X$ collisions at known values of E_{rel} involving UF_6^- molecules of initial U, J_0 distributions.

Excited UF_6^- molecules can dissociate into three low-lying product channels as illustrated in Fig. 1:

$$i=1: \quad (UF_6^-)^* \rightarrow UF_5^- + F, \quad U_{0,1} = 4.3 \pm 0.5 \text{ eV} \ ,$$

$$i=2: \quad (UF_6^-)^* \rightarrow UF_5 + F^-, \quad U_{0,2} = 4.7 \pm 0.3 \text{ eV} \ ,$$

$$i=3: \quad (UF_6^-)^* \rightarrow UF_6 + e, \quad U_{0,3} = 5.2 \pm 0.5 \text{ eV} \ ,$$

where the $U_{0,i}$ represent threshold internal energies and are taken from experimental sources.[2,3] The experimental uncertainties in the $U_{0,i}$, though large, are not all independent. The decomposition frequencies $k_i(U, J_0)$ of $(UF_6^-)^*$ molecules into product channels, i, can be obtained conveniently from the statistical ("quasiequilibrium") theory of Klots.[14] For the case in which a molecular spherical (or near spherical) top dissociates into a molecular spherical (or near spherical) top and an atom (or electron), Klots' expression for the decomposition frequency is

$$k_i(U, J_0) = \frac{\alpha_i}{h(2J_0+1)\rho_{vib}^{(UF_6^-)^*}(E_{vib})} \times \int_{\chi=0}^{U_i = U - U_{0,i}} \rho_{vib}^{Prod}(\chi) \sum_J \sum_L (2J+1) d\chi \ , \quad (5)$$

where h is Planck's constant; $\rho_{vib}^{(UF_6^-)^*}$ is the vibrational density of states of $(UF_6^-)^*$ at vibrational energy E_{vib}; χ, $\rho_{vib}^{Prod}(\chi)$, and J are the vibrational energy, vibrational density of states, and rotational angular momentum quantum number of the product spherical top molecule, respectively; L is the orbital angular momentum quantum number of the products; and α_i is the ratio of the symmetry numbers of UF_6^- and the product spherical top. The density of vibrational states of a polyatomic molecule can be approximated accurately by the method of Whitten and Rabinowitch[19] for $\epsilon \gg \epsilon_0$:

$$\rho_{vib}(\epsilon) = \left[(\epsilon + \epsilon_0)^{s-1}\right] \Big/ \left[(s-1)! \prod_i h\nu_i\right]$$

where ϵ = energy above the zero-point level, ϵ_0 = zero-point energy, s = number of vibrational degrees of freedom, and ν_i = vibrational frequencies. Because ρ_{vib} is such a strong function of energy, excited electronic states of UF_6^- and products need not be considered in our analysis because their vibrational densities of states at any given total energy are smaller than those of the respective electronic ground states. This simplification is central to the analysis since the species involved have many low-lying excited electronic states.

The restrictions on the angular momentum quantum numbers J and L in Eq. (5) are determined as follows: For the spherical top-atom channels ($i = 1, 2$), once a value of χ is chosen, the rotational energy E_{rot} of the product spherical top can range from 0 to $U - U_{0,i} - \chi$. Since

$$E_{rot} = B \cdot J(J+1) \quad (6)$$

for a spherical top where B is the rotational constant, the range of J is thereby defined. The range of L (if any) is defined by the triangle rule $|J - J_0| \leq L \leq J + J_0$ and the Langevin (polarizability) restriction on L_{max}[14]:

$$L_{max}(L_{max}+1) = \gamma (U - \chi - E_{rot})^{1/2} \ ,$$

where

$$\gamma = 2^{3/2} \mu e \alpha^{1/2} / \hbar^2$$

and where μ = the reduced mass of the CID products, e = electronic charge, and α = polarizability. For the electron detachment channel, only s and p electrons contribute appreciably so that $L = 0, 1$ and $J = J_0 \pm 1$, where J_0 is the $(UF_6^-)^*$ angular momentum quantum number.

Necessary inputs for the calculations of k_i are the threshold energies $U_{0,i}$,[2,3] the harmonic oscillator frequencies,[3,20] rotational constants,[3] and symmetry numbers[3,20] of UF_6^-, UF_5^-, and UF_5, and the dipole polarizations of UF_5 and F.[21] The uncertainties in these parameters are often severe. For example, some of the UF_6^- harmonic oscillator frequencies are obtained by assuming them to equal those of the isoelectronic species NpF_6; whereas the UF_5^- frequencies are assumed to equal those of UF_5. Thus, even if Eq. (5) were exactly correct, the various calculated values of k_i would be highly uncertain. Once the $k_i(U, J_0)$ have been determined, the branching ratios R_i can be obtained from the formula

$$R_i = k_i \Big/ \sum_j k_j \ . \quad (7)$$

We have computed $k_i(U, J_0)$, $i = 1, 2, 3$, numerically for internal $(UF_6^-)^*$ energies under 15 eV and a variety of angular momenta. Figure 9 depicts the $k_i(U, J_0 = 0)$. The dissociation frequencies shown are strongly dependent on internal energy, ranging from less than 10^5 sec^{-1} near threshold to 10^{14} sec^{-1} at 15 eV. Note that the detachment channel is correctly predicted to be a minor

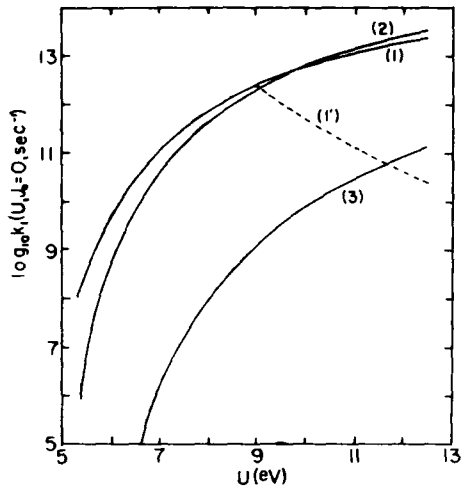

FIG. 9. Calculated decomposition frequencies $k_i(U, J_0 = 0)$ are plotted as a function of the internal energy U for channels $i = 1$ ($UF_5^- + F$), $i = 1'$ ($UF_5^- + F$, allowing for secondary decomposition of UF_5^-), $i = 2$ ($UF_5 + F^-$), and $i = 3$ ($UF_6 + e$).

one. The computed values of $k_i(U, J_0)$ are also dependent on J_0. Increasing J_0 tends to decrease the dissociation frequencies, especially near threshold.

To compare our theoretical and experimental results, we have calculated the branching ratios R_i. For all values of angular momentum considered, R_3 (the detachment channel branching ratio) is $\lesssim 0.01$ and increases with increasing energy. This is in qualitative agreement with the experiment. However, the actual numerical values appear to be lower than experimental values for any reasonably assumed internal energy distributions of $(UF_6^-)^*$. The ratio of channel (1), UF_5^-, to channel (2), (F^-), products as a function of E_{rel} is a salient feature of our experimental results. The theory can "reproduce" this feature if it is reasonably assumed that the $(UF_6^-)^*$ rotational energy is a fixed percentage of total internal energy. In Fig. 10(a), we have plotted calculated values of $k_i(U, J_0)$, assuming E_{rot} to be held fixed at 17% of the internal energy U. In Fig. 10(b) the ratio k_1/k_2 is then plotted against $(UF_6^-)^*$ internal energy with rotational energy $E_{rot} = 0.17U$. Note that the ratio decreases strongly at energies just above threshold ($\simeq 6$ eV) and then levels off. The analogous experimental plot shows a similar dependence of $\sigma(UF_5^-)/\sigma(F^-)$ on collision energy E_{rel}. In this plot (Fig. 6) the leveling off occurs at $E_{rel} \simeq 15$–20 eV. One would expect the plot of the above ratio versus internal energy of $(UF_6^-)^*$ to be sharper than Fig. 6, because the range of $(UF_6^-)^*$ internal energies for any collision energy will certainly lie below E_{rel}. The exact shape of the theoretical curve is a function of the percentage of total internal energy of $(UF_6^-)^*$ assumed to be rotational energy. Still, for E_{rot} equal to a variety of fixed percentages of U, the qualitative feature remains: the ratio of UF_5^- to F^- products decreases with increasing U, at first sharply and then more slowly (until $U \simeq 9$ eV where secondary decomposition of UF_5^- occurs). Despite the wide uncertainties in the parameters used in the calculations, this reproduction of the experimental feature must be regarded as a success of the theory. It stems from two facets of the calculation. At lower energies the lower threshold energy of $UF_5^- + F$ production dominates; whereas, at higher energies the higher polarizability of UF_5 (compared with F) results in more $UF_5 + F^-$ states being "counted" in Eq. (5). The absolute k_1/k_2 predictions, though tantalizingly close to the experimental branching ratios for $E_{rot} = 0.17U$ and any reasonable U distribution, should not be taken as seriously.

Finally, the theoretical results show that the threshold for detachment is larger by several electron volts than the threshold for CID. The transit time in the collision chamber of the total cross section apparatus is ~ 1 μsec. Consequently, the value of k_i for any channel must reach $\sim 10^6$ sec^{-1} before products can be detected. Depending on the amount of angular momentum possessed by $(UF_6^-)^*$, the decomposition frequency for detachment reaches this value at internal energies U of 1.5–3.0 eV in excess of the CID channels. If E_{rot} is once again held fixed at 17% of U, the figure is ~ 2.75 eV. This is in good agreement with the threshold experimental results depicted in Fig. 7 where CID onsets at a *collision* energy of 2–3 eV below detachment.

V. SUMMARY

Measurements of the absolute total cross sections for collisional decomposition of UF_6^- into its three lowest-lying asymptotic channels have been made for collision energies ranging from below threshold up to 500 eV laboratory energy. The targets used in the experimental

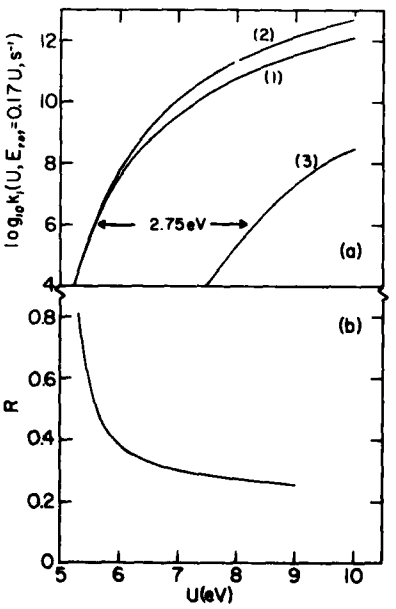

FIG. 10. (a) Calculated decomposition frequencies $k_i(U, J_0)$ for $E_{rot} = 0.17U$. See Fig. 9 for an explanation of the symbols. Note that for $k \simeq 10^6$ sec^{-1}, the internal energy necessary for detachment is 2.7 eV greater than that for CID. (b) The branching ratio between channels (1) and (2) above as a function of internal energy for $E_{rot} = 0.17U$.

studies were the rare gases Ne, Ar, Kr, and Xe. In addition, the product velocity spectra for one of the decomposition channels have been determined for the highest collision energies.

The salient features of the experimental findings are (i) the cross sections for the collisional electron detachment of UF_6^- are quite small and are no more than a few percent of the total decomposition cross sections over the range of energies investigated; (ii) the cross sections for the less endoergic dissociation channel (UF_5^- + F) are smaller than those for the channel ($UF_5 + F^-$) for relative collision energies above about 10 eV; (iii) the general features of all the cross sections, when plotted as a function of the relative collision energy, are independent of whichever rare gas target is involved; (iv) the threshold energy for electron detachment is about 2–3 eV greater than that for the dissociation channel ($UF_5 + F^-$); (v) the velocity spectra indicate that the collision that leads to the principal decomposition channel ($UF_5 + F^-$) is most probably several electron volts more endoergic than the minimum endoergicity required for the dissociation to occur.

These results have been analyzed with a two-step collision model where collisional excitation of UF_6^- is followed by unimolecular decomposition which is target independent. The branching ratios for the unimolecular decomposition have been calculated by using a statistical formulation, which has been discussed previously by Klots.[14] Although the details of the original collisional excitation of UF_6^- are not incorporated in the model, the statistical predictions for unimolecular decomposition are in qualitatively good agreement with the experimental observations.

ACKNOWLEDGMENTS

This work was supported in part by the U.S. Department of Energy, Division of Chemical Sciences and the Air Force Office of Scientific Research (W and M), and by the U.S. Department of Energy, under Contract W-7405-eng-26 with Union Carbide Corporation (ORNL).

[1]P. F. Dittner and S. Datz, J. Chem. Phys. 68, 2451 (1978).
[2]J. L. Beauchamp, J. Chem. Phys. 64, 929 (1976).
[3]R. N. Compton, J. Chem. Phys. 66, 4478 (1977).
[4]B. P. Mathur, E. W. Rothe, and G. P. Reck, J. Chem. Phys. 67, 777 (1977).
[5]B. K. Annis and S. Datz, J. Chem. Phys. 69, 2553 (1978).
[6]J. A. D. Stockdale, R. J. Warmack, and R. N. Compton, Chem. Phys. Lett. 63, 621 (1979).
[7]M. Boring, J. H. Wood, and J. W. Moskowitz, J. Chem. Phys. 61, 3800 (1974).
[8]M. Boring, Chem. Phys. Lett. 46, 242 (1977).
[9]P. J. Hay, W. R. Wadt, L. R. Khan, R. C. Raffenetti, and D. H. Phillips, J. Chem. Phys. 71, 1767 (1979).
[10]D. D. Koelling, D. E. Ellis, and R. J. Bartlett, J. Chem. Phys. 65, 331 (1976).
[11]M. Boring and J. H. Wood, J. Chem. Phys. 71, 32 (1979).
[12]B. K. Annis and J. A. D. Stockdale, J. Chem. Phys. 74, 297 (1981).
[13]A portion of the present work was reported on previously: R. L. Champion, L. D. Doverspike, E. Herbst, S. Haywood, B. K. Annis, and S. Datz, XIth ICPEAC, Kyoto, 1979, p. 618 of Abstracts of Contributed Papers.
[14]C. E. Klots, J. Phys. Chem. 75, 1526 (1971); Z. Naturforsch. Teil A 27, 553 (1972); J. Chem. Phys. 64, 4269 (1976); Chem. Phys. Lett. 38, 61 (1976).
[15]B. T. Smith, W. R. Edwards, L. D. Doverspike, and R. L. Champion, Phys. Rev. A 18, 945 (1978).
[16]The assumptions associated with this rather simple model have been discussed previously, e.g., E. Herbst, K. A. Mulholland, R. L. Champion, and L. D. Doverspike, J. Chem. Phys. 67, 5074 (1977).
[17]J. T. Cheung and S. Datz, J. Chem. Phys. 71, 1814 (1979); 73, 3159 (1980).
[18]P. J. Chantry, J. Chem. Phys. 55, 2746 (1971).
[19]G. Z. Whitten and B. S. Rabinowitch, J. Chem. Phys. 41, 1883 (1964).
[20]B. J. Krohn, W. B. Person, and J. Overand, J. Chem. Phys. 65, 969 (1976).
[21]R. R. Teachout and R. T Pack, At. Data 3, 195 (1971); Natl. Bur. Stand. (U.S.) Circ. 537 (1953). The polarizability of UF_5 is approximated to be equal to that of UF_6.

END

DATE
FILMED
1-82

DTIC